INSTITUTE OF PHYSICS PUBLISHING JOURNAL OF OPTICS A: PURE AND APPLIED OPTICS
J. Opt. A: Pure Appl. Opt. **8** (2006) 142–148 doi:10.1088/1464-4258/8/2/006

Computer modelling of tungsten–tellurite photonic crystal optical fibres for parametric fibre devices

V O Sokolov, V G Plotnichenko, V O Nazaryants and E M Dianov

Fiber Optics Research Center, General Physics Institute of the Russian Academy of Sciences, 38 Vavilov Street, Moscow 119991, Russia

E-mail: sokolov@fo.gpi.ac.ru

Received 7 September 2005, accepted for publication 28 November 2005
Published 11 January 2006
Online at stacks.iop.org/JOptA/8/142

Abstract
Computer modelling of light propagation in optical fibres formed by vacancies in two-dimensional periodic lattices is performed using the MIT Photonic-Bands package to calculate fully vectorial definite-frequency eigenmodes of Maxwell's equations with periodic boundary conditions in a plane-wave basis. The lattices consist of cylindrical holes in bulk glass or of glass tubes with the holes and gaps between the tubes filled with air. Single-site hexagonal and square lattices, often studied both theoretically and experimentally and used in manufacturing silica glass-based photonic crystal optical fibres, are considered. The calculations are carried out for the $80TeO_2$–$20WO_3$ tungsten–tellurite glass-based fibres with the refractive index frequency dispersion taken into account. The numerical solutions are analysed by the effective mode area approach. The modelled dependences of fundamental mode dispersion on geometrical parameters of the fibres are used to suggest tungsten–tellurite photonic crystal fibres of several types for parametric devices.

Keywords: optical fibre applications, optical fibre dispersion, periodic structure, photonic crystal optical fibre, tellurite glass

1. Introduction

Photonic crystal fibres have opened a new stage in fibre optics. Nowadays the terminology concerning optical fibres with spatially periodic refractive index is not yet established. Such terms as Bragg, photonic crystal, holey, microstructure etc fibres are used. In this paper we consider optical fibres formed only by a fragment of two-dimensional photonic crystal with the spatially periodic refractive index in transversal plane and a defect in the central area. The defect forms fibre core, and the surrounding refractive index lattice forms a fibre cladding. For definiteness such optical fibre will be referred to as photonic crystal fibre (PCF).

Owing to the photonic crystal cladding, PCFs are known to possess a number of properties distinguishing them from usual optical fibres. Thus, PCFs can be single mode in a very wide wavelength range [1]. The value and slope of dispersion can vary considerably depending on geometrical PCF parameters allowing one, for example, to shift the dispersion zero point to essentially shorter wavelengths in comparison with the glass material dispersion, to obtain a low-slope dispersion in a wide enough wavelength range, or a required dispersion value at a given wavelength [2–5]. Scale transformation of geometrical parameters of a single-mode PCF enables the effective mode area to be varied in a wide range (practically up to two orders of magnitude), thus controlling nonlinear effects in the fibres [4, 6, 7].

Recently the PCFs based on silica (v-SiO_2) glass have been actively investigated and manufactured (see, for example, [7, 8]). However, many applications require materials with higher values of refractive index and nonlinear susceptibilities than those of v-SiO_2. In particular, TeO_2-based glasses are known to possess such properties (see, for example, [9, 10]). Recent trends are toward a successful use of tellurite glasses for manufacturing PCFs [11, 12].

 © 2006 IOP Publishing Ltd Printed in the UK

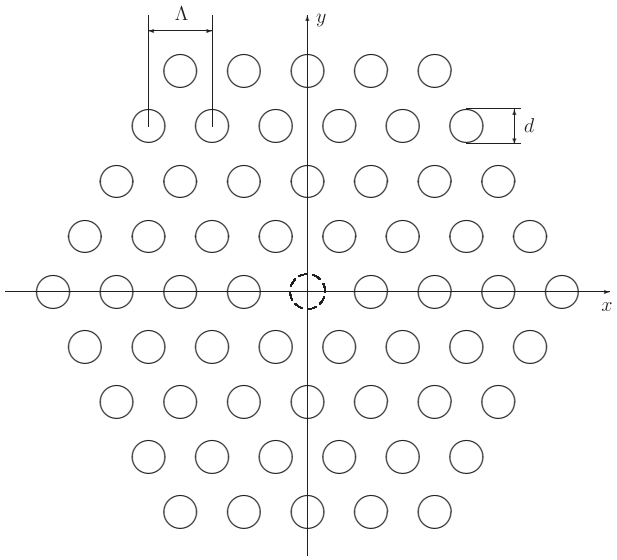

Figure 1. HH PCF: hexagonal lattice of holes in glass with a vacancy (one filled hole is shown by a dashed line).

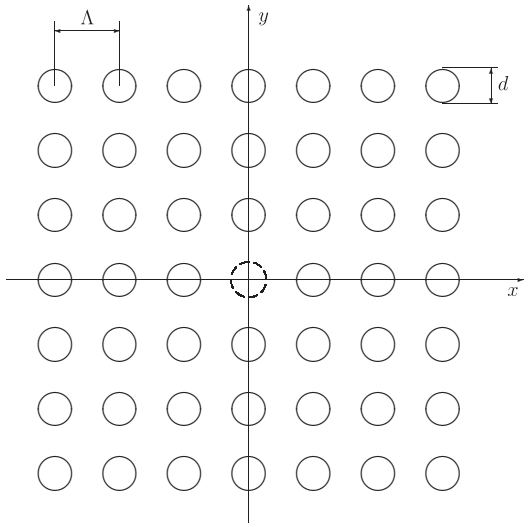

Figure 2. SH PCF: square lattice of holes in glass with a vacancy (one filled hole is shown by a dashed line).

The primary goal of this work is to find the PCF structure both simple and most applicable in parametric fibre devices (amplifiers etc) operating at a pumping wavelength near 1.55 μm. The main requirements for such PCFs are known to be as follows:

- high value of the third-order dielectric susceptibility;
- small enough fibre core diameter to produce high enough power density in the core;
- zero dispersion of the effective refractive index near the operating wavelength or, in a more general case, the possibility to obtain a designated level of dispersion in a certain wavelength range;
- single-mode fibres.

The first requirement can be satisfied well by using the tellurite glass-based PCFs. To satisfy the others we performed the computer modelling of light propagation in the PCFs formed by a point defect in a two-dimensional periodic lattice consisting of either cylindrical holes in bulk glass or glass tubes, the holes and gaps between the tubes being filled with air ($\varepsilon = 1$). We considered single-site hexagonal and square lattices most often studied both theoretically and experimentally and recently used in manufacturing silica glass-based PCFs. As for the defects, we used both a single vacancy (an absent lattice site, i.e. a single hole in the glass bulk, or a single tube, filled with the same glass) and the same vacancy with the nearest neighbours being holes with increased diameter (or tubes with increased inner diameter) as compared with the diameter of the lattice holes (or inner diameter of the tubes, respectively). Fragments of the lattices in the vicinity of the vacancy are shown in figures 1–4.

All calculations were performed for tungsten–tellurite ($80TeO_2$–$20WO_3$) glass-based PCFs (for brevity, the $80TeO_2$–$20WO_3$ glass is termed below 'tellurite glass'), with the frequency dispersion of the glass dielectric constant taken into account. The two-pole Sellmeier approximation of the

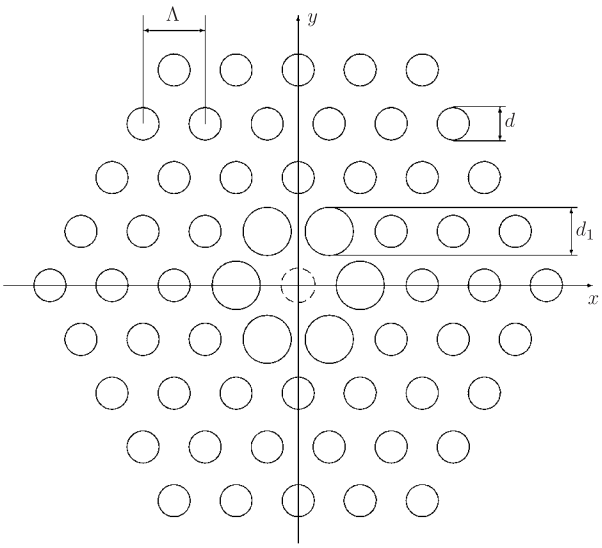

Figure 3. HH1 PCF: hexagonal lattice of holes in glass with a vacancy (one filled hole is shown by a dashed line) surrounded by first-neighbour holes with increased diameter.

wavelength dependence of the glass dielectric constant in the transparency region was taken from [13]:

$$\varepsilon(\lambda) = A + B(1 - C\lambda^{-2})^{-1} + D(1 - E\lambda^{-2})^{-1}$$

with λ being the wavelength in micrometres, $A = 2.490\,9866$, $B = 1.951\,5037$, $C = 5.674\,0339 \times 10^{-2}$ μm^2, $D = 3.021\,2592$, $E = 225$ μm^2.

The following abbreviations are used below for the PCFs under consideration:

HH PCF is formed by a filled central hole in a simple hexagonal lattice of cylindrical holes in glass;

SH PCF is formed by a filled central hole in a simple square lattice of cylindrical holes in glass;

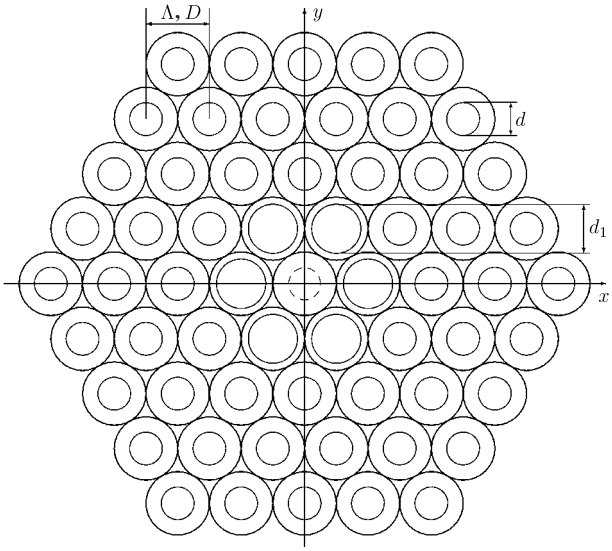

Figure 4. HT1 PCF: hexagonal lattice of tubes with a vacancy (one filled tube is shown by a dashed line) surrounded by first-neighbour tubes with increased inner diameter.

HH1 PCF is formed by a filled central hole in a simple hexagonal lattice of cylindrical holes in glass surrounded by first-neighbour holes with increased diameter;

HT1 PCF is formed by a filled tube in a simple hexagonal lattice of cylindrical glass tubes surrounded by first-neighbour tubes with increased inner diameter.

The following designations are used in the paper:

Λ is the refractive index lattice constant (in the lattice of tubes Λ is obviously equal to the outer tube diameter, D),
d is the diameter of holes in bulk glass or inner tube diameter,
d_1 is the diameter of holes in bulk glass (inner tube diameter) in the first row around the vacancy (if d_1 differs from d),
ε is the dielectric constant of glass,
λ is the incident light wavelength (in vacuum, $\lambda = 2\pi c/\omega$),
ω is the incident light frequency,
c is the vacuum light velocity,
β is the fibre propagation constant,
$\mathbf{k}$ is the wavevector, and
$A_{\text{eff}}^{(i)}$ is the effective area of the ith mode.

The light is supposed to propagate along the z axis transversely to the refractive index lattice plane, xy.

Effective mode area, A_{eff}, is determined according to [14] by

$$A_{\text{eff}}^{(i)}(\lambda) = \left[\int I^{(i)}(\mathbf{r}_\perp)\,\mathrm{d}^2 r_\perp\right]^2 \left[\int \left[I^{(i)}(\mathbf{r}_\perp)\right]^2 \mathrm{d}^2 r_\perp\right]^{-1}$$

where $\mathbf{r}_\perp$ are the coordinates in the refractive index lattice plane, xy, and $I^{(i)}(\mathbf{r}_\perp)$ is the ith mode intensity.

Fibre numerical aperture, NA, is determined in accordance with [15] as NA $= \sin\vartheta$ in the far-field limit, with ϑ being the half-divergence angle of the Gaussian field. The numerical aperture is related to the effective mode area as follows [15]:

$$\mathrm{NA} \approx \left(1 + \pi\frac{A_{\text{eff}}}{\lambda^2}\right)^{-1/2}.$$

Effective refractive index is as usual

$$n_{\text{eff}} = \beta\frac{c}{\omega}.$$

Effective dispersion is given as

$$M_{\text{eff}} = -\frac{\lambda}{c}\frac{\mathrm{d}^2 n_{\text{eff}}(\lambda)}{\mathrm{d}\lambda^2}.$$

2. Modelling of photonic crystal fibres

All calculations are performed with the help of the MIT Photonic-Bands package [16] (MPB in what follows), a freely available program to compute fully vectorial definite-frequency eigenmodes of Maxwell's equations with periodic boundary conditions in a plane-wave basis.

The system of source-free Maxwell's equations for a dielectric with $\varepsilon = \varepsilon(\mathbf{r})$ is known to be reduced to one vectorial equation and one scalar equation for the magnetic field $\mathbf{H}(t, \mathbf{r})$ only [17]:

$$\nabla \times \left[\frac{1}{\varepsilon(\mathbf{r})}\nabla \times \mathbf{H}(t,\mathbf{r})\right] = -\frac{1}{c^2}\frac{\partial^2 \mathbf{H}(t,\mathbf{r})}{\partial t^2}$$
$$\nabla \cdot \mathbf{H}(t,\mathbf{r}) = 0. \qquad (1)$$

In the medium with periodic dielectric constant the electromagnetic fields satisfy the Bloch's theorem. The fields with definite frequency ω, i.e. with time-dependence $\exp(-\mathrm{i}\omega t)$, can be represented in such a dielectric in the form

$$\mathbf{H}(t,\mathbf{r}) = \mathbf{H}_{\mathbf{k}}(\mathbf{r})\mathrm{e}^{\mathrm{i}(\mathbf{kr}-\omega t)},$$

where $\mathbf{k}$ is the Bloch wavevector and $\mathbf{H}_{\mathbf{k}}(\mathbf{r})$ is a periodic function completely determined by its values in the (first) Brillouin zone. For such fields and a dielectric, the equations (1) become a linear eigenproblem in the Brillouin zone

$$\mathbf{A}_{\mathbf{k}}\mathbf{H}_{\mathbf{k}}(\mathbf{r}) = \left(\frac{\omega}{c}\right)^2 \mathbf{H}_{\mathbf{k}}(\mathbf{r}), \qquad (2)$$

where $\mathbf{A}_{\mathbf{k}} \equiv (\nabla + \mathbf{k}) \times \varepsilon^{-1}(\nabla + \mathbf{k}) \times$ is the Hermitian operator. Representing the H field in a finite basis, one transforms equation (2) to an eigenvalue equation for the Hermitian matrix. In the MPB package the plane-wave basis is used as

$$\mathbf{H}_{\mathbf{k}}(\mathbf{r}) = \sum_{\mathbf{b}} \mathbf{h}_{\mathbf{k}+\mathbf{b}}\mathrm{e}^{\mathrm{i}(\mathbf{k}+\mathbf{b})\mathbf{r}},$$

cut at large enough values of the reciprocal lattice vectors, $\mathbf{b}$. The cut-off radius determining the number of basis functions is chosen from the required calculation accuracy (the computer representation of a real number, by default). In view of periodicity, the decomposition coefficients, $\mathbf{h}_{\mathbf{k}+\mathbf{b}}$, depend only on $\mathbf{k} + \mathbf{b}$ sums.

Features of the numerical methods and their realization in the MPB and instructions for package users are described in detail in [16, 18].

To calculate the PCF formed by a point defect in a two-dimensional periodic refractive index lattice, the supercell method was used [18]. In the described calculations a 12×12-sized lattice constant and a vacancy in the supercell centre

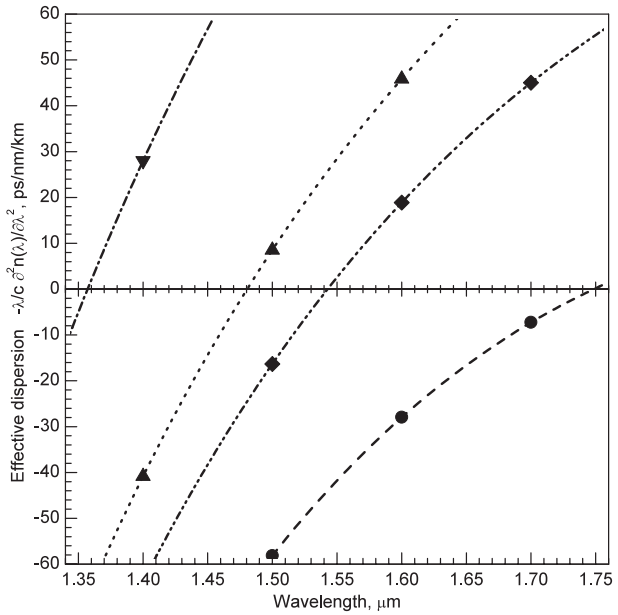

Figure 5. The effective fundamental mode dispersion in HH PCF with $\Lambda = 1.50\ \mu$m: ● $d/\Lambda = 0.40$, ♦ $d/\Lambda = 0.52$, ▲ $d/\Lambda = 0.60$, ▼ $d/\Lambda = 0.80$.

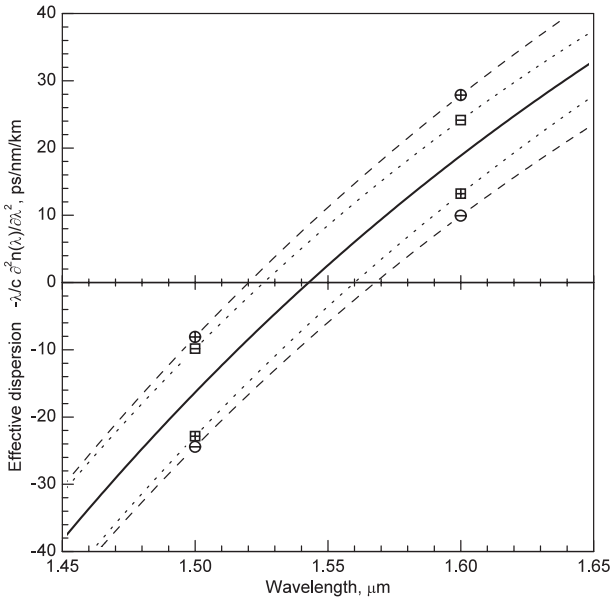

Figure 6. Influence of geometrical parameters on the effective fundamental mode dispersion in HH PCF with $\Lambda_0 = 1.50\ \mu$m, $d_0/\Lambda_0 = 0.52$: ⊞ $\Lambda = 1.05\Lambda_0$, ⊟ $\Lambda = 0.95\Lambda_0$, ⊕ $d = 1.05d_0$, ⊖ $d = 0.95d_0$.

were used. Calculations were performed for a single **k** point, namely the Brillouin zone centre (the Γ point) of the supercell. Such an approach enables studying the modes localized in the vicinity of the vacancy with a diameter of the order of 4Λ. Our calculation has proved that all the localized modes studied have a significantly smaller diameter of their localization area, and hence are practically not influenced by the periodic boundary conditions for the supercell.

Calculations of the PCFs of each type were performed for several lattice constant values, $1\ \mu\text{m} \lesssim \Lambda \lesssim 3\ \mu$m, and at each lattice constant value for several values of the relative hole diameter (or inner tube diameter), $d = 0.2, 0.4, 0.6$ and 0.8. In the case of the HH1 and HT1 fibres calculations were performed as well for several values of relative diameter of the first row holes (or inner diameter of the first row tubes), $d_1 = 0.6, 0.7$ and 0.8. For each set of geometrical parameters the effective refractive index of the fundamental (first) mode of the PCF, its effective dispersion, the effective area of the three lowest (twofold degenerated with respect to polarization) modes of the PCF and the numerical aperture for the fundamental mode were calculated. Based on the data obtained in the calculation, the optimal values of the geometrical parameters were derived to meet all the above-mentioned requirements of PCFs for the parametric devices. Thus several tellurite glass PCFs were selected with the properties described below. In order to determine the stability of the PCF properties in relation to possible variations of geometrical parameters in manufacturing process, additional calculations were performed for each of these PCFs with the geometrical parameters differing from the optimal ones by ±5%. All the calculations were carried out for one and the same set of wavelengths from the range $1.0 \leqq \lambda \leqq 2.4\ \mu$m.

3. Main results and discussion

HH PCF with the lattice constant $\Lambda = 1.50\ \mu$m. Wavelength dependences of the effective fundamental mode dispersion are shown in figure 5 for several values of the relative hole diameter. As is seen in the figure, for $d = 0.52\Lambda = 0.78\ \mu$m this PCF has zero effective dispersion at the wavelength $\lambda = 1.545\ \mu$m, the dispersion slope in the vicinity of this wavelength being approximately 0.37 ps nm^{-2} km^{-1}. At the operating wavelength $\lambda = 1.55\ \mu$m the effective area of the fundamental mode is found to be $A_{\text{eff}}^{(1)} = 1.3096\Lambda^2 \approx 3.0\ \mu\text{m}^2$ and the numerical aperture is approximately NA ≈ 0.60. Such a PCF is single mode at $\lambda \gtrsim 1.1\ \mu$m.

Figure 6 shows changes in the effective dispersion curve with the PCF geometrical parameters varying. With the transversal sizes or the lattice hole relative diameter being scaled within the ±5% range, the position of the effective dispersion zero is shifted approximately by ±10 and ∓15 nm, respectively, and the dispersion slope changes approximately by 0.01 ps nm^{-2} km^{-1}.

SH PCF with the lattice constant $\Lambda = 1.20\ \mu$m. As is seen from the wavelength dependences of the effective fundamental mode dispersion shown in figure 7 for several values of the relative hole diameter, for $d = 0.53\Lambda = 0.64\ \mu$m, the effective dispersion becomes zero at $\lambda = 1.551\ \mu$m, and the dispersion slope in the vicinity of this wavelength is approximately 0.28 ps nm^{-2} km^{-1}. The effective area of the fundamental mode turns out to be $A_{\text{eff}}^{(1)} = 0.7665\Lambda^2 \approx 2.5\ \mu\text{m}^2$ and the numerical aperture is NA ≈ 0.47 at the operating wavelength $\lambda = 1.55\ \mu$m. In this case the PCF is single mode at $\lambda \gtrsim 0.9\ \mu$m.

Change in the effective dispersion curve with the geometrical parameters of the PCF varying within the ±5% range is shown in figure 8. Owing to the transversal size

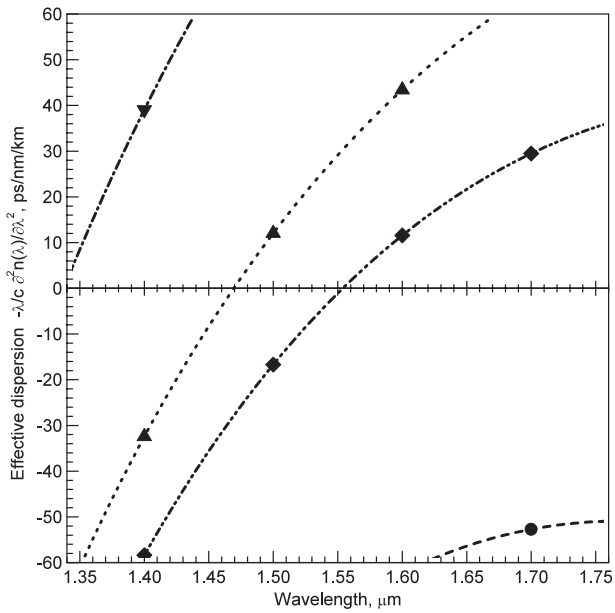

Figure 7. The effective fundamental mode dispersion in SH PCF with $\Lambda = 1.20\ \mu$m: ● $d/\Lambda = 0.40$, ♦ $d/\Lambda = 0.53$, ▲ $d/\Lambda = 0.60$, ▼ $d/\Lambda = 0.80$.

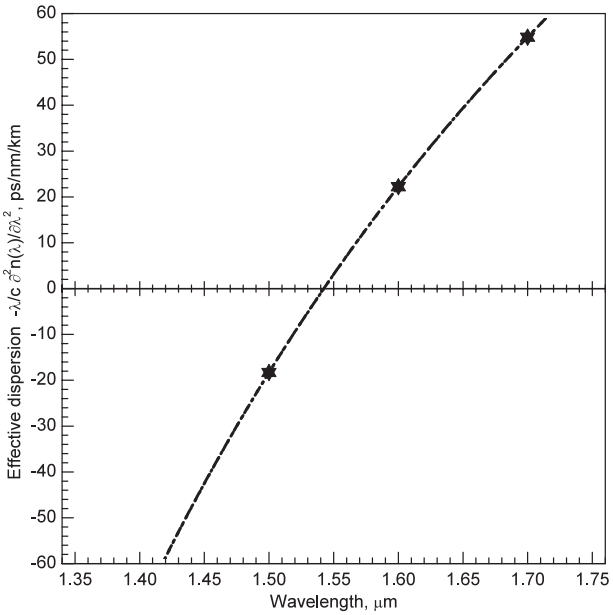

Figure 9. The effective fundamental mode dispersion in the HH1 PCF with $\Lambda = 2.20\ \mu$m, $d_1/\Lambda = 0.80$: ▲ $d/\Lambda = 0.60$, ▼ $d/\Lambda = 0.80$.

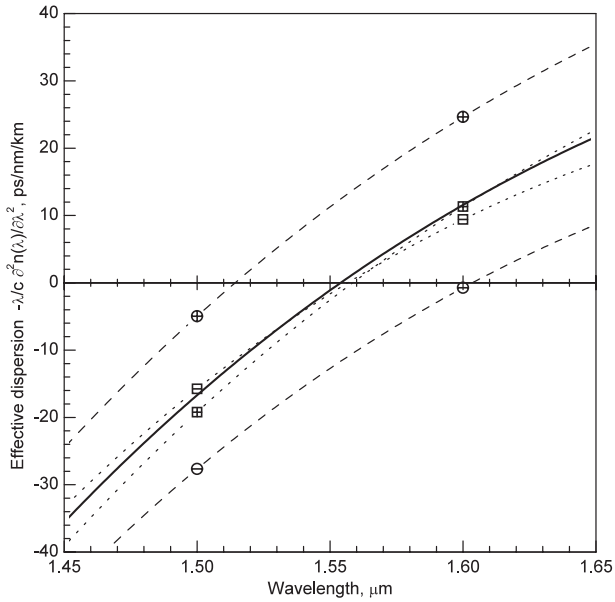

Figure 8. Influence of geometrical parameters on the effective fundamental mode dispersion in SH PCF with $\Lambda_0 = 1.20\ \mu$m, $d_0/\Lambda_0 = 0.53$: ⊞ $\Lambda = 1.05\Lambda_0$, ⊟ $\Lambda = 0.95\Lambda_0$, ⊕ $d = 1.05d_0$, ⊖ $d = 0.95d_0$.

scaling, the effective dispersion zero is shifted approximately by ±4 nm. With the relative diameter of lattice holes changing by ±5%, the dispersion zero point is shifted by ∓40 and ±50 nm, respectively. Change in the dispersion curve slope turns out to be about 0.02 and 0.05 ps nm^{-2} km^{-1}, respectively.

HH1 PCF with the lattice constant $\Lambda = 2.20\ \mu$m and relative diameter of the holes in the first row around the central filled hole $d_1 = 0.80\Lambda = 1.76\ \mu$m. The calculations have shown that in the wavelength range under consideration such structures possess light-guide properties only if the diameter of the lattice holes is large enough, namely, if $d \gtrsim 0.5\Lambda = 1.1\ \mu$m. The effective dispersion of the PCF fundamental mode is plotted against the wavelength in figure 9. Our calculations have revealed that the effective dispersion practically does not depend on the lattice hole diameter in the range $d \gtrsim 0.5\Lambda$, becoming zero at $\lambda = 1.542\ \mu$m with the slope about 0.40 ps nm^{-2} km^{-1}. At the operating wavelength $\lambda = 1.55\ \mu$m the effective fundamental mode area is found to be $A_{\text{eff}}^{(1)} = 0.7342\Lambda^2 \approx 3.6\ \mu$m^2, and the numerical aperture NA ≈ 0.41. So the PCF is single mode at $\lambda \gtrsim 1.1\ \mu$m for $d \lesssim 0.7\Lambda = 1.5\ \mu$m.

Figure 10 shows how the effective dispersion changes with the geometrical parameters of the PCF varying. As indicated above, changing of the relative diameter of the lattice holes in the range $d \gtrsim 0.5\Lambda$ does not influence the effective dispersion. Scaling of the transversal sizes through the ±5% range results in the dispersion zero point shifted by ±24 nm; the same variation of the diameter of the holes in the first row around the central filled hole shifts the dispersion zero by ∓24 nm. The slope of the dispersion curve changes less than by 0.01 ps nm^{-2} km^{-1} in both cases.

HT1 PCF with the lattice constant (outer tube diameter) $\Lambda = D = 2.70\ \mu$m and inner diameter of the tubes in the first row around the central filled tube $d_1 = 0.80\Lambda = 2.16\ \mu$m. According to the calculation results, in the wavelength range under consideration these PCFs possess light-guide properties for all values of inner diameter of the lattice tubes in the range of practical interest, $d \gtrsim 0.1\Lambda \approx 0.25\ \mu$m, and the PCF is single mode at $\lambda \gtrsim 0.8\ \mu$m for any $d \lesssim 0.3\Lambda \approx 0.80\ \mu$m. The effective dispersion of the PCF fundamental mode is shown versus wavelength in figure 11. In the range $d \gtrsim 0.1\Lambda$ the effective dispersion is virtually independent of the inner diameter of the lattice tubes. The dispersion turns to zero at

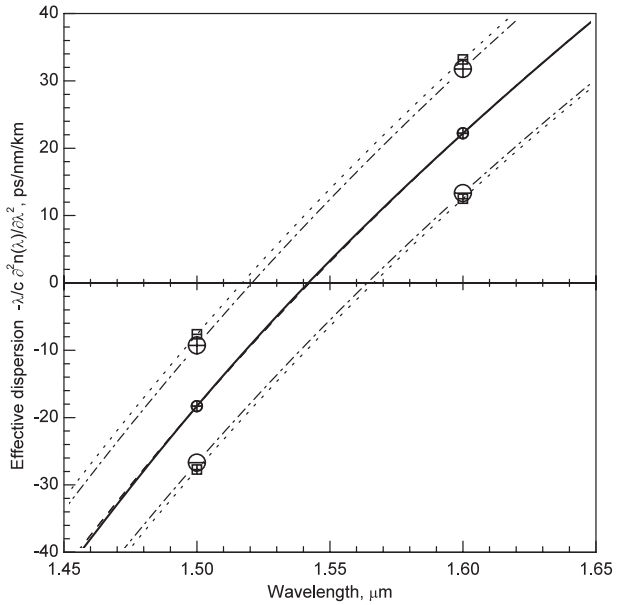

Figure 10. Influence of geometrical parameters on the effective fundamental mode dispersion in the HH1 PCF with $\Lambda_0 = 2.20$ μm, $d_0/\Lambda_0 = 0.60$, $d_{1_0}/\Lambda = 0.80$: $\boxplus$ $\Lambda = 1.05\Lambda_0$, $\boxminus$ $\Lambda = 0.95\Lambda_0$, $\oplus$ $d = 1.05d_0$, $\ominus$ $d = 0.95d_0$, $\oplus$ $d_1 = 1.05d_{1_0}$, $\ominus$ $d_1 = 0.95d_{1_0}$.

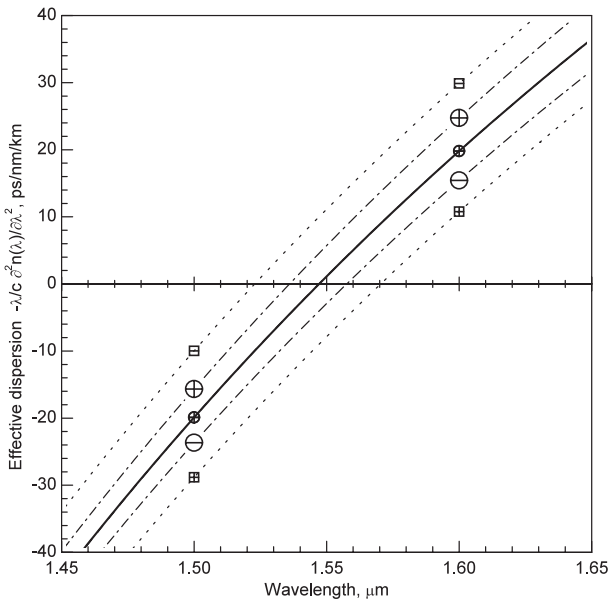

Figure 12. Influence of geometrical parameters on the effective fundamental mode dispersion in the HT1 PCF with $\Lambda_0 = 2.70$ μm, $d_0/\Lambda_0 = 0.20$, $d_{1_0}/\Lambda = 0.80$: $\boxplus$ $\Lambda = 1.05\Lambda_0$, $\boxminus$ $\Lambda = 0.95\Lambda_0$, $\oplus$ $d = 1.05d_0$, $\ominus$ $d = 0.95d_0$, $\oplus$ $d_1 = 1.05d_{1_0}$, $\ominus$ $d_1 = 0.95d_{1_0}$.

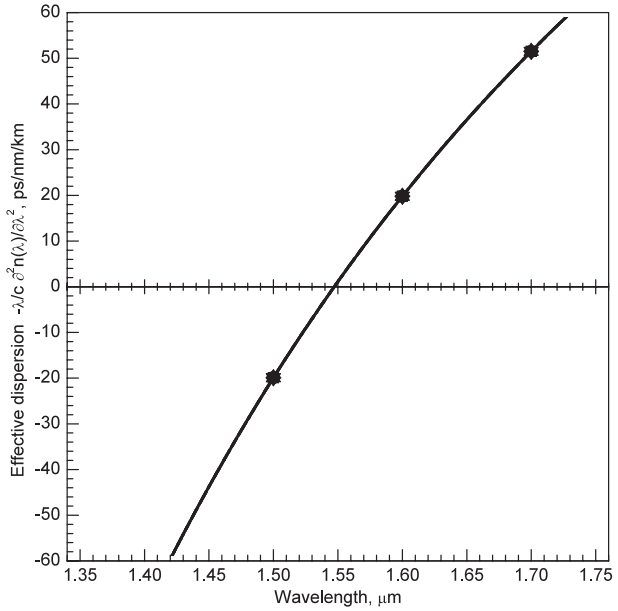

Figure 11. The effective fundamental mode dispersion in the HT1 PCF with $\Lambda = 2.70$ μm, $d_1/\Lambda = 0.80$: ● $d/\Lambda = 0.20$, ▲ $d/\Lambda = 0.40$, ▼ $d/\Lambda = 0.60$.

$\lambda = 1.548$ μm, the dispersion slope in the vicinity of this wavelength being about 0.40 ps nm^{-2} km^{-1}. At the operating wavelength, $\lambda = 1.55$ μm, the effective fundamental mode area is $A_{\text{eff}}^{(1)} = 0.4564\Lambda^2 \approx 3.3$ μm^2 and the numerical aperture is NA ≈ 0.42.

Figure 12 demonstrates the dependence of the effective dispersion on the PCF geometrical parameters. Again, variation of the inner relative diameter of the lattice tubes does not influence the effective dispersion, while either the transversal size scaling or changing of the inner diameter of the tubes in the first row around the central filled tube through the $\pm 5\%$ range leads to a shift of the dispersion zero point by approximately ± 22 and ∓ 10 nm, respectively. Again, change in the dispersion curve slope does not exceed 0.01 ps nm^{-2} km^{-1} in both cases.

Among all of the PCFs studied, the SH one has the lowest effective fundamental mode area, the least dispersion slope near the dispersion zero point (approximately 25% less than in other PCFs) and the dispersion curve most stable in relation to the transversal sizes scaling (the displacement of the dispersion zero point is approximately one-fifth that in other PCFs). On the other hand, the SH PCF has the worst stability of its dispersion zero point in relation to variation of the lattice hole diameter: displacement of the dispersion zero point is about twice as large as in other PCFs.

The distinctive feature of HH1 and HT1 PCFs with increased diameter of the holes (or inner diameter of the tubes) in the first row around the central filled hole (or tube) consists in that the dispersion curve is practically insensitive to variation of d, i.e. the diameter of the holes (or inner diameter of the tubes) forming the rest of the lattice (see figures 9 and 11). However, the diameter d determines the number of guided modes of the PCFs, the HH1 and HT1 PCFs being single mode only for low enough d values. The stability of the dispersion curve of both PCFs in relation to the transversal size scaling appears to be approximately identical and close to that of the HH PCF. On the other hand, the HT1 PCF turns out to be much more stable relative to the variation of the first-row hole diameter, d_1, than the HH1 one relative to variation of the inner first-row tube diameter. Thus, the displacement of the dispersion zero point is twice as small in the HT1 PCF as in the HH1 one. Obviously, this results from the stabilizing influence of air gaps between the tubes in the HT1 PCF.

The HH1 and HT1 PCFs turn out to have approximately the same effective fundamental mode areas, dispersion slopes and numerical apertures, the numerical aperture value of these PCFs appearing the lowest among all of the PCFs studied. On the other hand, the largest numerical aperture is found in the HH PCF.

4. Conclusion

In the present paper we consider the PCFs formed by point defects (a single vacancy and a vacancy with holes of increased diameter as the first nearest neighbours) in the two-dimensional single-site hexagonal and square lattices of either cylindrical holes in glass or glass tubes. The numerical modelling of these PCFs is performed for tungsten–tellurite glass $80TeO_2$–$20WO_3$ ($n \approx 2.11$ at $1.5\ \mu$m) with the refractive index frequency dispersion taken into account. Results of the calculations allow us to suggest several simple types of tungsten–tellurite PCFs for parametric fibre devices. Namely,

(i) A PCF formed by a filled central hole in a simple hexagonal lattice of cylindrical holes in glass (the centre-to-centre distance is $\Lambda = 1.50\ \mu$m; the hole diameter is $d = 0.78\ \mu$m). The fibre has a zero dispersion at $\lambda = 1.545\ \mu$m with the dispersion slope of about 0.37 ps nm^{-2} km^{-1}. It is single mode for the wavelengths $\lambda \gtrsim 1.1\ \mu$m with the effective fundamental mode area $A_{\mathrm{eff}}^{(1)} \approx 3.0\ \mu$m^2 and the numerical aperture NA ≈ 0.60 at the operating wavelength $1.55\ \mu$m.

(ii) A PCF formed by a filled central hole in a simple square lattice of cylindrical holes in glass (the centre-to-centre distance is $\Lambda = 1.20\ \mu$m; the hole diameter is $d = 0.64\ \mu$m). The fibre has a zero dispersion at $\lambda = 1.551\ \mu$m with the dispersion slope of about 0.28 ps nm^{-2} km^{-1}. The fibre is single mode for $\lambda \gtrsim 0.9\ \mu$m. At the operating wavelength, $1.55\ \mu$m, its effective fundamental mode area is $A_{\mathrm{eff}}^{(1)} \approx 2.5\ \mu$m^2 and the numerical aperture is NA ≈ 0.47.

(iii) A PCF formed by a filled central hole in a simple hexagonal lattice of cylindrical holes in glass (the centre-to-centre distance is $\Lambda = 2.20\ \mu$m; the diameter of the holes in the first row around the filled hole is $d_1 = 1.76\ \mu$m; the diameter of other holes is in the $1.1 \lesssim d \lesssim 1.5\ \mu$m range). For any diameter of the holes from the range mentioned above such a fibre has a zero dispersion at $\lambda = 1.542\ \mu$m with a dispersion slope of about 0.40 ps nm^{-2} km^{-1}, an effective area of the fundamental mode of $A_{\mathrm{eff}}^{(1)} \approx 3.6\ \mu$m^2 and a numerical aperture of NA ≈ 0.41 at the operating wavelength ($1.55\ \mu$m). The fibre is single mode for the wavelengths $\lambda \gtrsim 1.0\ \mu$m.

(iv) A PCF formed by a single filled tube in a simple hexagonal lattice of cylindrical glass tubes (the centre-to-centre distance (outer diameter) is $\Lambda = D = 2.70\ \mu$m^2, the inner diameter of the tubes in the first row around the filled tube is $d_1 = 2.16\ \mu$m^2 and the inner diameter of the other tubes is in the $0.25 \lesssim d \lesssim 0.80\ \mu$m range). For any inner diameter of the tubes in the range mentioned above this PCF has zero dispersion at $\lambda = 1.548\ \mu$m with the dispersion slope about 0.40 ps nm^{-2} km^{-1}, the effective fundamental mode area $A_{\mathrm{eff}}^{(1)} \approx 3.3\ \mu$m^2 and the numerical aperture NA ≈ 0.42 at the operating wavelength, $1.55\ \mu$m, being single mode for $\lambda \gtrsim 0.8\ \mu$m.

References

[1] Birks T A, Knight J C and Russell P St-J 1997 *Opt. Lett.* **22** 961
[2] Mogilevtsev D, Birks T A and Russell P St-J 1998 *Opt. Lett.* **23** 1662
[3] Bennett P J, Monro T M and Richardson D J 1999 *Opt. Lett.* **24** 1203
[4] Broderick N G R, Monro T M, Bennett P J and Richardson D J 1999 *Opt. Lett.* **24** 1395
[5] Ferrando A, Silvestre E, Moret J J and Andrés P 2000 *Opt. Lett.* **25** 790
[6] Knight J C, Birks T A, Gregan R F, Russell P St-J and de Sandro J-P 1998 *Electron. Lett.* **13** 1347
[7] Zheltikov A M 2004 *Phys. Usp.* **47** 69
[8] Eberly J H 2001 *Opt. Express* **9** 674
[9] El-Mallawany R A H 2002 *Tellurite Glasses Handbook* (New York: CRC Press)
[10] Stegeman R, Jankovic L, Kim H, Rivero C, Stegeman G, Richardson K, Delfyett P, Guo Y, Schulte A and Cardinal T 2003 *Opt. Lett.* **28** 1126
[11] Hu E S, Hsueh Y-L, Marhic M E and Kazovsky L G 2002 *Proc. 28th European Conf. on Optical Communication (Copenhagen, Denmark)* paper 3.2.3
[12] Mori A, Shikano K, Enbutsu K, Oikawa K, Naganuma K, Kato M and Aozasa S 2004 *Proc. 30th European Conf. on Optical Communication (Stockholm, Sweden)* paper 3.3.6
[13] Ghosh G 1995 *J. Am. Ceram. Soc.* **78** 2828
[14] Mortensen N A 2002 *Opt. Express* **10** 341
[15] Mortensen N A, Folkenberg J R, Skovgaard P M W and Broeng J 2002 *IEEE Photon. Technol. Lett.* **14** 1094
[16] Johnson S G and Joannopoulos J D 2001 *Opt. Express* **8** 173
[17] Landau L D and Lifshitz E M 1984 *Electrodynamics of Continuous Media* (Oxford: Pergamon)
[18] Johnson S G 2003 *The MIT Photonic-Bands Manual* Massachusetts Institute of Technology